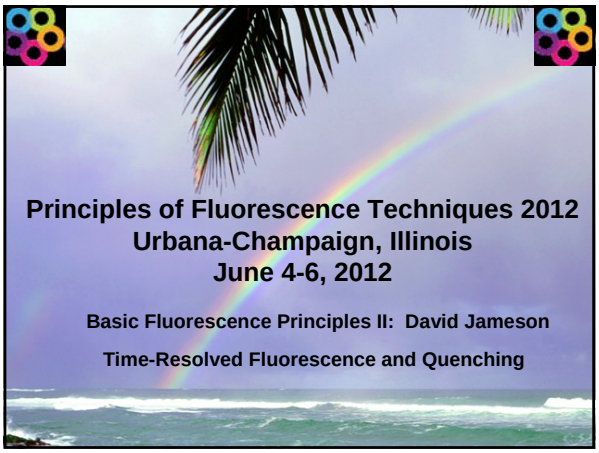
Principles of Fluorescence Techniques 2012
Urbana-Champaign, Illinois
June 4-6, 2012
Basic Fluorescence Principles II: David Jameson
Time-Resolved Fluorescence and Quenching

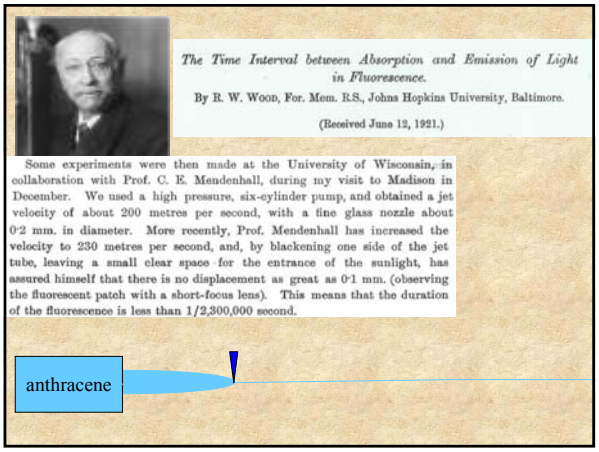
The Time Interval between Absorption and Emission of Light in Fluorescence.
By R. W. Wood, For. Mem. R.S., Johns Hopkins University, Baltimore.
(Received June 12, 1921.)
Some experiments were then made at the University of Wisconsin, in collaboration with Prof. C. E. Mendenhall, during my visit to Madison in December. We used a high pressure, six-cylinder pump, and obtained a jet velocity of about 200 metres per second, with a fine glass nozzle about 0·2 mm. in diameter. More recently, Prof. Mendenhall has increased the velocity to 230 metres per second, and, by blackening one side of the jet tube, leaving a small clear space for the entrance of the sunlight, has assured himself that there is no displacement as great as 0·1 mm. (observing the fluorescent patch with a short-focus lens). This means that the duration of the fluorescence is less than 1/2,300,000 second.
anthracene

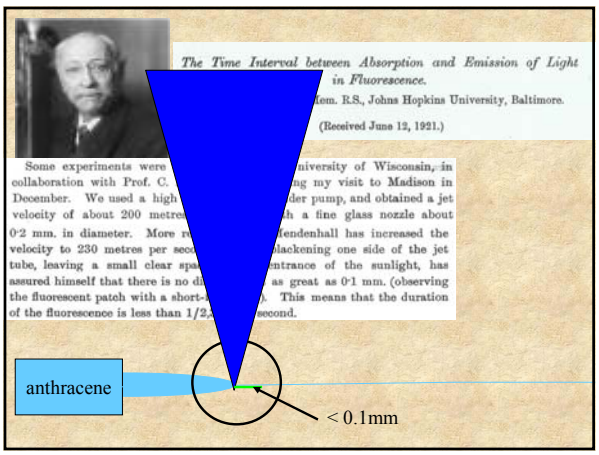
The Time Interval between Absorption and Emission of Light in Fluorescence.
(Received June 12, 1921.)
anthracene
< 0.1mm

The Time Interval between Absorption and Emission of Light in Fluorescence.

By R. W. Wood, For. Mem. R.S., Johns Hopkins University, Baltimore.

(Received June 12, 1921.)

Some experiments were then made at the University of Wisconsin, in collaboration with Prof. C. E. Mendenhall, during my visit to Madison in December. We used a high pressure, six-cylinder pump, and obtained a jet velocity of about 200 metres per second, with a fine glass nozzle about 0·2 mm. in diameter. More recently, Prof. Mendenhall has increased the velocity to 230 metres per second, and, by blackening one side of the jet tube, leaving a small clear space for the entrance of the sunlight, has assured himself that there is no displacement as great as 0·1 mm. (observing the fluorescent patch with a short-focus lens). This means that the duration of the fluorescence is less than 1/2,300,000 second.

i.e. < 435ns

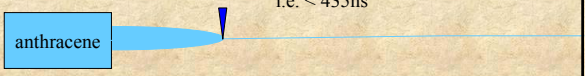

This work was followed by a report by Philip Gottling in 1923 who used a Kerr Cell – as originally suggested by Lord Rayleigh in 1905.

THE DETERMINATION OF THE TIME BETWEEN EXCITATION AND EMISSION FOR CERTAIN FLUORESCENT SOLIDS

By Philip F. Gottling

Abstract

Time lag between excitation and emission of fluorescence by barium platino-cyanide and rhodamine.—The work begun in 1921 by R. W. Wood on the measurement of fluorescent intervals and phosphorescent times has been continued. The method of Abraham and Lemoine, somewhat modified, was used for determining the very short periods of time involved. The fluorescent light is polarized and then passed through a condenser, containing nitrobenzene as dielectric, which had begun to be discharged when the illuminating spark started. The later the light arrives the lower the average field of the condenser and the smaller the angular setting of the analyzing nicol to match the two images produced by a double image prism. The apparatus was calibrated by means of light reflected from a mirror at different distances from the spark. The interval of time between the occurrence of a spark and the emission of the fluorescent light excited by that spark, was found to be $(2.12 \pm .01) \times 10^{-8}$ sec. for barium platino-cyanide and $(2.11 \pm .14) \times 10^{-8}$ sec. for rhodamine.

He found 21.1 ns for a solution of rhodamine in acetone, acetic acid and glycerol. Possibly he was observing a combination of fluorescence and phosphorescence

Ein Fluorometer.
Apparat zur Messung von Fluoreszenzabklingungszeiten.

Von E. Gaviola in Berlin.

Mit 9 Abbildungen. (Eingegangen am 24. März 1927.)

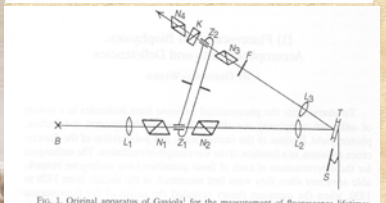

Fig. 1. Original apparatus of Gaviola' for the measurement of fluorescence lifetimes, described in text. *B*, Source of exciting light; *T*, cuvette containing the fluorescent solution; *S*, mirror.

Enrique Gaviola

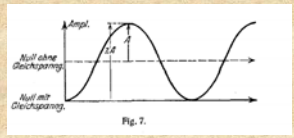

Fig. 7.

Farbstoff	Abklingungszeiten in Wasser Sekunden	in Glycerin Sekunden	in Meth.-Alkohol Sekunden
Uranin	$4{,}5 \cdot 10^{-9}$	$4{,}4 \cdot 10^{-9}$	—
Fluorescein	—	—	$5{,}0 \cdot 10^{-9}$
Rhodamin B	$2{,}0 \cdot 10^{-9}$	$4{,}2 \cdot 10^{-9}$	—
Rhodulin Orange	2,7	4,3	—
Erythrosin	1,8	2,4	$2{,}6 \cdot 10^{-9}$
Tetrajodfluor. Na	1,0	2,0	2,2
Eosin 5 B	1,9	—	3,4
Uranylsulfat	—	—	1,3
Uranylsulfat in Schwefelsäure	—	—	1,9
Chinisarin in Pentan	—	—	2,9
Uranglas	—	—	$>15{,}0$
Rubinkristall	—	—	$>15{,}0$

What is meant by the "lifetime" of a fluorophore???

Although we often speak of the properties of fluorophores as if they are studied in isolation, such is not usually the case.

Absorption and emission processes are almost always studied on *populations* of molecules and the properties of the supposed typical members of the population are deduced from the macroscopic properties of the process.

In general, the behavior of an excited population of fluorophores is described by a familiar rate equation:

$$\frac{dn^*}{dt} = -n^* \Gamma + f(t)$$

where n^* is the number of excited elements at time t, Γ is the rate constant of emission and f(t) is an arbitrary function of the time, describing the time course of the excitation . The dimensions of Γ are sec^{-1} (transitions per molecule per unit time).

If excitation occurs at t = 0, the last equation, takes the form:

$$\frac{dn^*}{dt} = -n^* \Gamma$$

and describes the decrease in excited molecules at all further times. Integration gives:

$$n^*(t) = n^*(0) \exp(-\Gamma t)$$

The lifetime, τ, is equal to Γ^{-1}

If a population of fluorophores are excited, the lifetime is the time it takes for the number of excited molecules to decay to 1/e or 36.8% of the original population according to:

$$\frac{n^*(t)}{n^*(0)} = e^{-t/\tau}$$

In pictorial form: $\frac{n^*(t)}{n^*(0)} = e^{-t/\tau}$

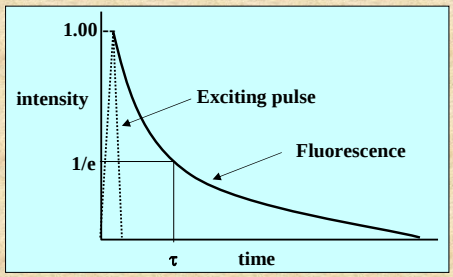

The lifetime and quantum yield for a given fluorophore is often dramatically affected by its environment.

Examples of this fact would be NADH, which in water has a lifetime of ~0.4 ns but bound to dehydrogenases can be a long as 9 ns.

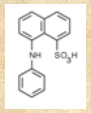

ANS in water is ~100 picoseconds but can be 8 – 10 ns bound to proteins

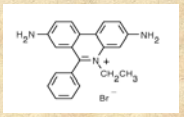

Ethidium bromide is 1.8 ns in water, 22 ns bound to DNA and 27ns bound to tRNA

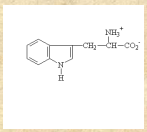

The lifetime of tryptophan in proteins ranges from ~0.1 ns up to ~8 ns

Excited state lifetimes have traditionally been measured using either the *impulse* response or the *harmonic* response method. In principle both methods have the same information content. These methods are also referred to as either the "time domain" method or the "frequency domain" method.

In the *impulse (*or pulse) method, the sample is illuminated with a short pulse of light and the intensity of the emission versus time is recorded. Originally these short light pulses were generated using *flashlamps* which had widths on the order of several nanoseconds. Modern laser sources can now routinely generate pulses with widths on the order of picoseconds or shorter.

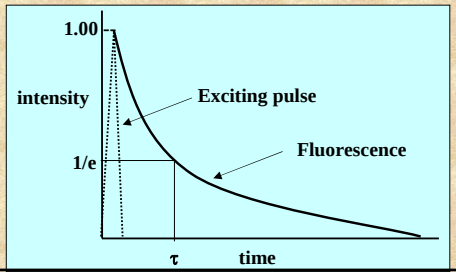

As shown in the intensity decay figure, the *fluorescence* lifetime, t , is the time at which the intensity has decayed to 1/e of the original value. The decay of the intensity with time is given by the relation:

$$I_t = \alpha e^{-t/\tau}$$

Where I_t is the intensity at time t, α is a normalization term (the pre-exponential factor) and τ is the lifetime.

It is more common to plot the fluorescence decay data using a logarithmic scale as shown here.

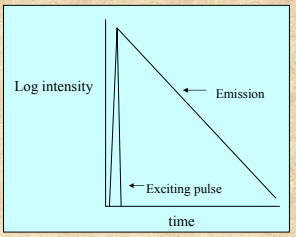

If the decay is a single exponential and if the lifetime is long compared to the exciting light then the lifetime can be determined directly from the slope of the curve.

If the lifetime and the excitation pulse width are comparable some type of *deconvolution* method must be used to extract the lifetime.

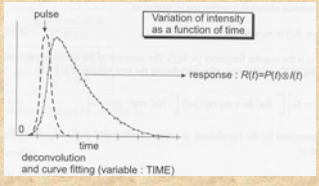

Great effort has been expended on developing mathematical methods to "deconvolve" the effect of the exciting pulse shape on the observed fluorescence decay.

With the advent of very fast laser pulses these deconvolution procedures became less important for most lifetime determinations, although they are still required whenever the lifetime is of comparable duration to the light pulse.

If the decay is multiexponential, the relation between the intensity and time after excitation is given by:

$$I(t) = \sum_i \alpha_i e^{-t/\tau_i}$$

One may then observe data such as those sketched below:

Here we can discern at least two lifetime components indicated as τ_1 and τ_2 . This presentation is oversimplified but illustrates the point.

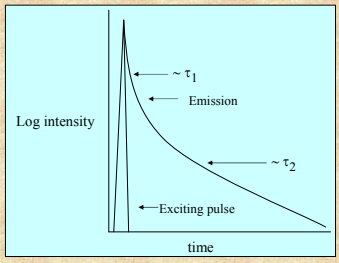

Here are pulse decay data on anthracene in cyclohexane taken on an IBH 5000U Time-correlated single photon counting instrument equipped with an LED short pulse diode excitation source.

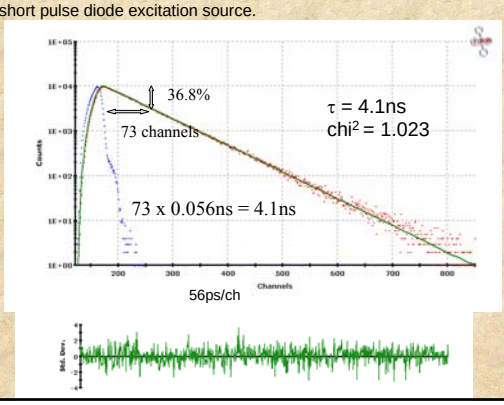

In the harmonic method (also known as the phase and modulation or frequency domain method) a continuous light source is utilized, such as a laser or xenon arc, and the intensity of this light source is modulated sinusoidally at high frequency as depicted below. Typically, an *electro-optic* device, such as a *Pockels cell* is used to modulate a continuous light source, such as a CW laser or a xenon arc lamp. Alternatively, LEDs or laser diodes can be directly modulated.

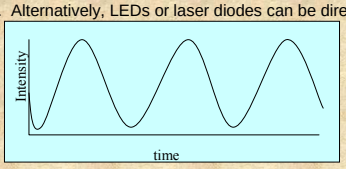

In such a case, the excitation frequency is described by:

$$E(t) = Eo\,[1 + M_E \sin \omega t]$$

E(t) and Eo are the intensities at time t and o, M_E is the modulation factor which is related to the ratio of the AC and DC parts of the signal and ω is the angular modulation frequency.
$\omega = 2\pi f$ where f is the linear modulation frequency

Due to the persistence of the excited state, fluorophores subjected to such an excitation will give rise to a modulated emission which is shifted in phase relative to the exciting light as depicted below.

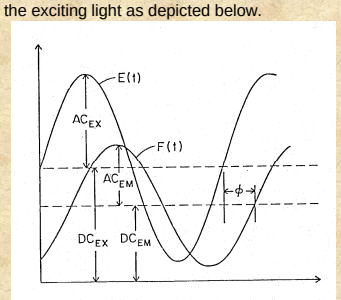

This sketch illustrates the phase delay (ϕ) between the excitation, E(t), and the emission, F(t). Also shown are the AC and DC levels associated with the excitation and emission waveforms.

One can demonstrate that:

$$F(t) = Fo\,[1 + M_F \sin(\omega t + \phi)]$$

This relationship signifies that measurement of the phase delay, ϕ, forms the basis of one measurement of the lifetime, τ. In particular one can demonstrate that:

$$\tan \phi = \omega\tau$$

The *modulations* of the excitation (M_E) and the emission (M_F) are given by:

$$M_E = \left(\frac{AC}{DC}\right)_E \quad \text{and} \quad M_F = \left(\frac{AC}{DC}\right)_F$$

The *relative modulation*, M, of the emission is then:

$$M = \frac{(AC/DC)_F}{(AC/DC)_E}$$

τ can also be determined from M according to the relation: $M = \dfrac{1}{\sqrt{1+(\omega\tau)^2}}$

Using the *phase shift* and *relative modulation* one can thus determine a *phase lifetime* (τ_P) and a *modulation lifetime* (τ_M).

If the fluorescence decay is a single exponential, then τ_P and τ_M will be equal at all modulation frequencies.

If, however, the fluorescence decay is multiexponential then $\tau_P < \tau_M$ and, moreover, the values of both τ_P and τ_M will depend upon the modulation frequency, i.e.,

$$\tau_P(\omega_1) < \tau_P(\omega_2) \quad \text{if} \quad \omega_1 > \omega_2$$

To get a feeling for typical phase and modulation data, consider the following data set.

Frequency (MHz)	τ_P (ns)	τ_M (ns)
5	6.76	10.24
10	6.02	9.70
30	3.17	6.87
70	1.93	4.27

These differences between τ_P and τ_M and their frequency dependence form the basis of the methods used to analyze for lifetime heterogeneity, i.e., the component lifetimes and amplitudes.

In the case just shown, the actual system being measured was a mixture of two fluorophores with lifetimes of 12.08 ns and 1.38 ns, with relative contributions to the total intensity of 53% and 47% respectively.

Here must must be careful to distinguish the term *fractional contribution to the total intensity* (usually designated as f) from α, the pre-exponential term referred to earlier. The relation between these two terms is given by:

$$f_i = \frac{\alpha_i \tau_i}{\sum_j \alpha_j \tau_j}$$

where j represents the sum of all components. In the case just given then, the ratio of the pre-exponential factors corresponding to the 12.08 ns and 1.38 ns components is approximately 1/3. In other words, there are three times as many molecules in solution with the 1.38 ns lifetime as there are molecules with the 12.08 ns lifetime.

Multifrequency phase and modulation data are usually presented as shown below:

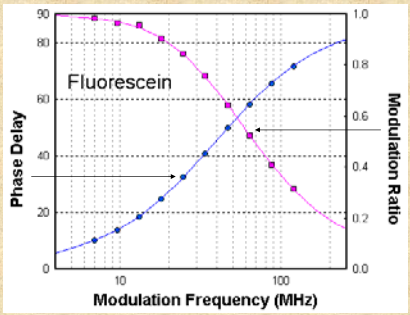

The plot shows the frequency response curve (phase and modulation) of Fluorescein in phosphate buffer pH 7.4 acquired on an ISS Chronos using a 470 nm LED. The emission was collected through a 530 high pass filter. The data is best fitted by a single exponential decay time of 4 ns.

In addition to decay analysis using discrete exponential decay models, one may also choose to fit the data to *distribution* models. In this case, it is assumed that the excited state decay characteristics of the emitting species actually results in a large number of lifetime components. Shown below is a typical lifetime distribution plot for the case of single tryptophan containing protein – human serum albumin.

The distribution shown here is Lorentzian but depending on the system different types of distributions, e.g., Gaussian or asymmetric distributions, may be utilized. This approach to lifetime analysis is described in: Alcala, J. R., E. Gratton and F. G. Prendergast. Fluorescence lifetime distributions in proteins. *Biophys. J. 51*, 597-604 (1987).

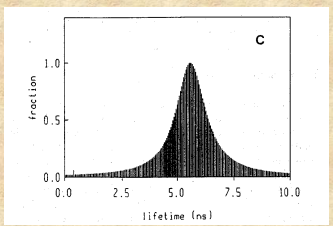

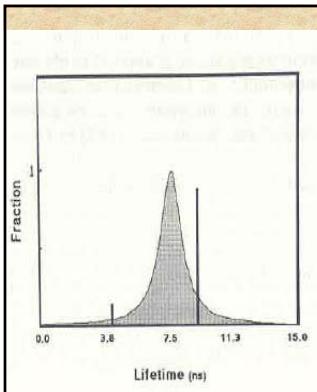

FIGURE 4. Continuous distribution (Lorentzian) lifetime analysis for methylanthraniloyl-GDP bound to the N-ras, P21 protein product (20°C). Calculated lifetime and full width at half-maximum were 7.7 and 1.1 nsec, respectively. The vertical dotted lines represent a two-component discrete lifetime fit to the same data: τ_1 = 8.5 nsec, 86% of the intensity, and τ_2 = 3.9 nsec. The χ^2 values were similar in both cases.

Another popular lifetime analysis method – based on Information Theory - is the *Maximum Entropy Method* (MEM). In this method no *a priori* intensity decay model is assumed.

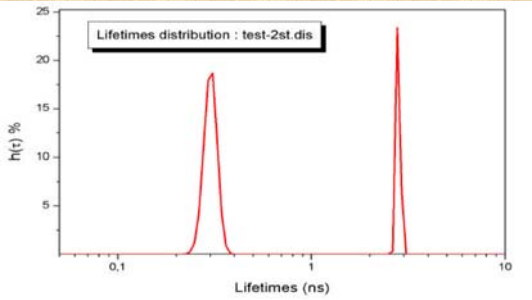

Jean-Claude Brochon
Maximum entropy method of data analysis in time-resolved spectroscopy.
Methods Enzymol. 1994;240:262-311.

Wavelength dependent lifetime data can be used to resolve individual spectra in a mixture

Gratton, E. and Jameson, D.M. (1985)
Anal. Chem. 57:1694-1697. New Approach to Phase and Modulation Resolved Spectra.

Mixture: Lifetimes were 10.8ns, 4.3ns and 0.9ns

Spectra of individual components

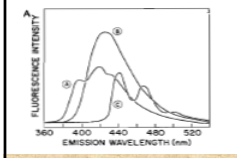

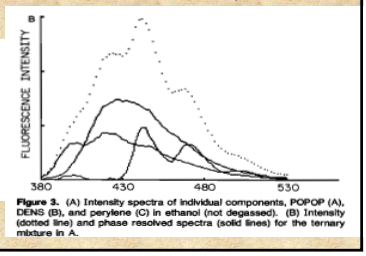

Figure 3. (A) Intensity spectra of individual components, POPOP (A), DENS (B), and perylene (C) in ethanol (not degassed). (B) Intensity (dotted line) and phase resolved spectra (solid lines) for the ternary mixture in A.

Global Analysis

In Global Analysis one can link decay parameters across many data sets which often allows for a more robust analysis

Example of the application of Global Analysis

Binding of Ethidium-Bromide to Transfer RNA

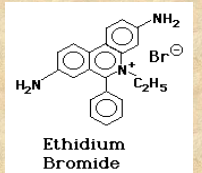

Ethidium Bromide

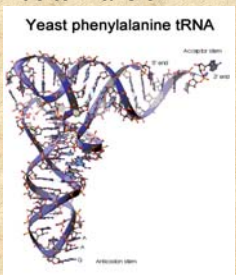

Ethidium bromide can intercalate into nucleic acid structures
It binds well to both DNA and RNA

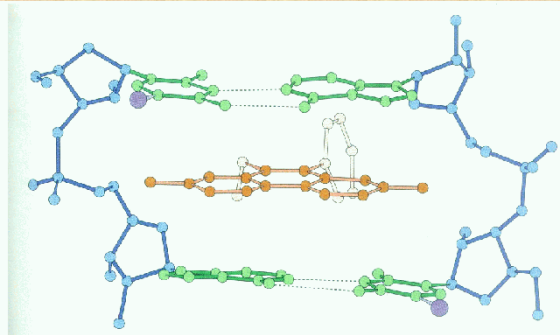

Fluorescence investigations of EB - tRNA interactions, carried out for more than 30 years, have indicated a "strong" binding site and one or more "weak, non-specific" binding sites.

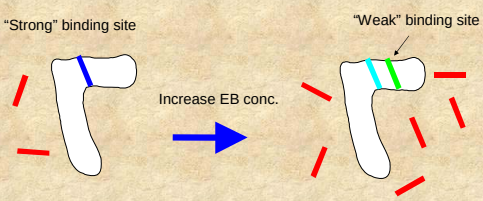

Question: What are the lifetimes of the strong and the weak binding sites???

If the tRNA is in excess only one EB will bind to the "strong" binding site which has a K_d of around 1 micromolar (under these conditions a single exponential decay of 27ns is observed). If the EB/tRNA ratio is increased, one or more additional EB's will bind and the question is: What are the lifetimes of EB bound to different sites on tRNA?" Shown below are phase and modulation data for a solution containing 124 μM yeast $tRNA^{phe}$ and 480 μM EB

The phase and modulation data were first fit to a single exponential component shown as the solid lines in the top plot. The residuals for this fit are shown in the bottom plot.

In this case τ = 18.49 ns and the χ^2 value was 250.

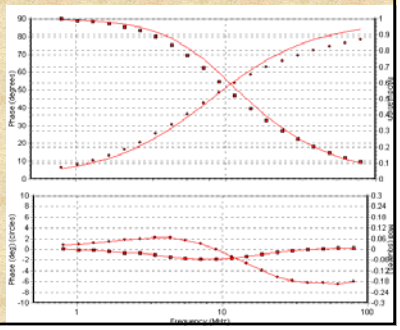

The data were then fit to a 2-component model shown here In this case the two lifetime components were 22.71 ns with a fractional intensity of 0.911 and 3.99 ns with a fractional intensity of 0.089.

The χ^2 for this fit was 3.06 (note the change in scale for the residual plot compared to the first case shown).

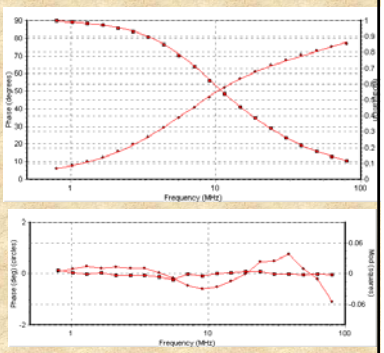

A 3-component model improves the fit still more. In this case

τ_1 = 24.25 ns, f_1 = 0.83

τ_2 = 8.79 ns, f_2 = 0.14

τ_3 = 2.09 ns, f_3 = 0.03

χ^2 = 0.39.

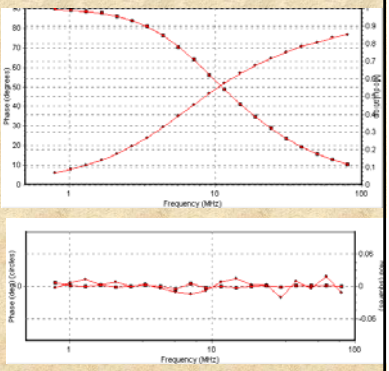

Adding a fourth component – with all parameters free to vary - does not lead to a significant improvement in the χ^2. In this case one finds 4 components of 24.80 ns (0.776), 12.13ns (0.163), 4.17 ns (0.53) and 0.88 ns (0.008).

But we are not using all of our information! We can actually fix some of the components in this case. We know that **free EB** has a lifetime of **1.84 ns** and we also know that the lifetime of **EB bound to the "strong" tRNA binding site** is **27 ns**. So we can fix these in the analysis. The results are four lifetime components of 27 ns (0.612), 18.33 ns (0.311), 5.85 ns (0.061) and 1.84 ns (0.016). The χ^2 improves to 0.16.

We can then go one step better and carry out **"Global Analysis"**.
In Global Analysis, multiple data sets are analyzed simultaneously and different parameters (such as lifetimes) can be "linked" across the data sets. The important concept in this particular experiment is that the lifetimes of the components stay the same and only their fractional contributions change as more ethidioum bromide binds.

In this system, 8 data sets, with increasing EB/tRNA ratios, were analyzed. Some of the data are shown below for EB/tRNA ratios of 0.27 (circles), 1.34 (squares), 2.41 (triangles) and 4.05 (inverted triangles).

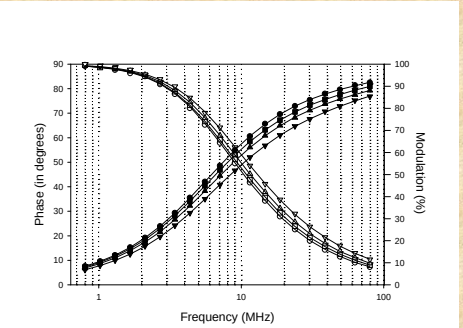

Global Analysis on seven data sets fit best to the 4 component model with two fixed components of 27ns and 1.84ns and two other components of 17.7ns and 5.4ns.

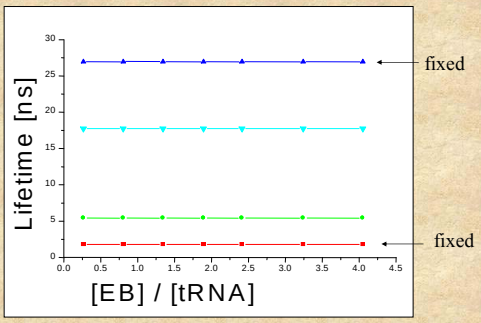

As shown in the plot below, as the EB/tRNA ratio increases the fractional contribution of the 27ns component decreases while the fractional contributions of the 17.7ns and 5.4ns components increase.

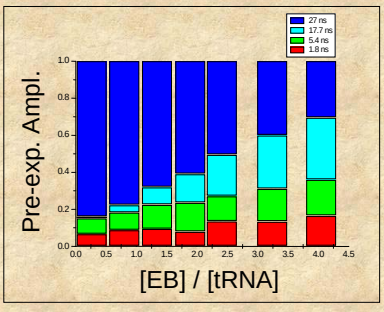

The Model

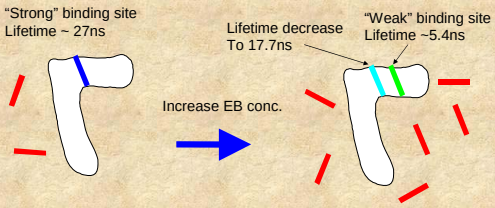

Question:
Is the drop in the lifetime of the "strong" binding site due to a change in tRNA conformation or energy transfer???

Answer: ???

Later in this workshop you'll learn about Fluorescence Lifetime Imaging or FLIM

In FLIM, lifetime data are obtained through a microscope - lifetime data is acquired at each pixel in the image

Lifetime data is more robust than intensity since it does not depend on how many fluorescent molecules are present

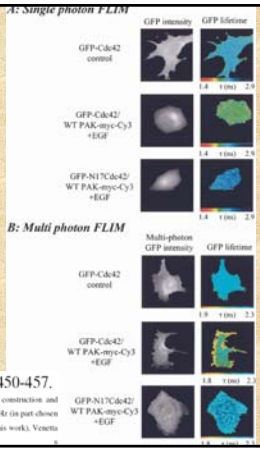

B. D. Venetta, *Rev. Sci. Instrum.*, 1959, **30**, 450-457.

In 1959 Venetta" described the construction and operation of a phase fluorometer coupled to a microscope. Using a frequency of 5.8 MHz (in part chosen due to the availability of FM transformers in televisions which could be salvaged for this work), Venetta was able to measure a lifetime of 2.7 ns for proflavin bound to the nuclei of tumor cells.

Introduction to Phasors

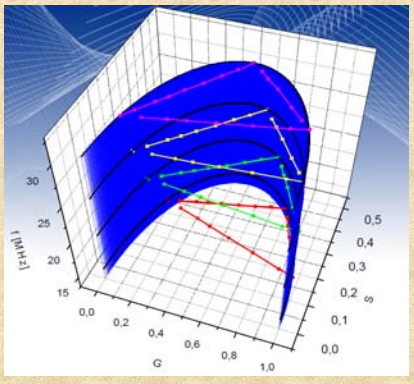

Resolution of the Fluorescence Lifetimes in a Heterogeneous System by Phase and Modulation Measurements

Gregorio Weber

Department of Biochemistry, School of Chemical Sciences, University of Illinois, Urbana, Illinois 61801 (Received: August 12, 1980)

A closed-form procedure is described for the determination of the decay constants and the relative contributing intensities of the N independent components of a heterogeneous fluorescence emission employing measurements of the phase shift and relative modulation of the total fluorescence at N appropriate harmonic excitation frequencies. At each frequency the phase and modulation measurements yield the real part of the Fourier transform of the fluorescence impulse response, G, and its imaginary part, S. It is shown that the moments of a distribution of the lifetimes are linear combinations of the Gs (zero and even moments) or the Ss (odd moments), and the rule for the construction of the coefficients of G and S in these linear combinations is derived. The classical de Prony method is used to obtain the lifetimes and fractional contributions of the components from the moments. For binary and ternary mixtures the numerical computations required are trivial. In the present state of the art, the lifetimes of the components of a binary mixture should be derivable with a loss in precision somewhat smaller than 1 order of magnitude with respect to the overall measured lifetimes.

$$G_\tau = M_\tau \cos \Phi_\tau = [(1 + (\omega_1\tau_1^2)^{-1})(1 + (\omega_1\tau_1 M)^2)]^{-1/2} \quad (9)$$

$$S_\tau = M_\tau \sin \Phi_\tau = G_\tau\omega_1\tau_1^2 \quad (10)$$

$$G(\omega) = \int_0^\infty I(t) \cos \omega t \, dt$$

$$S(\omega) = -\int_0^\infty I(t) \sin \omega t \, dt \quad (55)$$

APPLIED SPECTROSCOPY REVIEWS, 20(1), 55–106 (1984)

The Measurement and Analysis of Heterogeneous Emissions by Multifrequency Phase and Modulation Fluorometry

DAVID M. JAMESON
Department of Pharmacology
The University of Texas Health Science Center at Dallas
Dallas, Texas 75235

ENRICO GRATTON
Department of Physics
University of Illinois at Urbana–Champaign
Urbana, Illinois 61801

ROBERT D. HALL
Laboratory of Molecular Biophysics
National Institute of Environmental Health Sciences
Research Triangle Park
North Carolina 27709

APPENDIX 2. PHASE AND MODULATION LIFETIME RELATIONS

We have asserted that a heterogeneous emitting population, in the absence of excited state reaction, will demonstrate a phase lifetime which is always less than the modulation lifetime. The algebraic demonstration of this fact is somewhat cumbersome [11, 68]. We present here a brief and more intuitive demonstration of the phenomenon.

One may make a simple geometrical representation of the phase delay and relative modulation as shown in Fig. 11. Here we depict a vector of length M making an angle ϕ with the x-axis where ϕ represents the phase delay and M the relative modulation. Since for a single exponential decay we have the relation $M = \cos \phi$, the endpoint of the vector is constrained to be on the circle of radius 1/2 with a center at (1/2, 0). The intercept of the extension of this vector with the line through $x = 1$ equals $\omega\tau$ since $\tan \phi = \omega\tau$. This circle is universal for single exponential systems irrespective of the lifetime or modulation frequency. We note that the X and Y intercepts of the vector correspond to our previously defined G and S functions (since $G = M \cos \phi$ and $S = M \sin \phi$).

Figure 12 represents the case of two exponential decays with phase delays and relative modulations of ϕ_1, ϕ_2 and M_1, M_2, respectively. These decays contribute to the total emission intensity decay with fractional weights of f_1 and f_2, respectively. The total fluorescence observed is represented by the vector sum, M_τ of the two components and gives an observed phase delay of ϕ_τ. Again we see that the intercept of the extension of the M vector with the $x = 1$ line corresponds to $\omega\tau^\phi$ (since $\tan \phi = \omega\tau^\phi$). The value of $\omega\tau^\phi$, however, corresponds to the line segment BD. This observation follows from the fact that the triangle OAB,

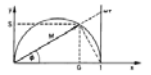

FIG. 11. Geometrical representation of phase delay (ϕ) and modulation ratio (M) for a single exponential decay.

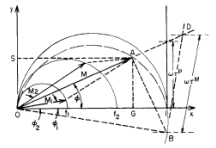

FIG. 12. Geometrical representation of phase delay (ϕ) and modulation ratio (M) for a double exponential decay.

The mathematical equivalence of impulse and harmonic response data does not, however, mean that practical differences between the methods do not exist. One important difference which is seldom mentioned concerns the fact that the impulse response technique does not permit the analysis of photons originating over the complete time domain. The time domain data are in essence truncated and obliged to be between somewhat arbitrary limits in addition to falling into time bins of finite width. In the harmonic response, regardless of the modulating frequency, the time information content of the emitted photons is not sacrificed. Moreover, in the single photon counting pulse technique one is permitted to observe at best only one photon per exciting pulse (to avoid statistical pileup effects this limit is, in fact, reduced) whereas in the harmonic response approach all the photons contribute to the measured signal. This later fact confers a sensitivity to the harmonic method which compares favorably with that of single photon counting, contrary to popular belief.

Journal of Fluorescence, Vol. 1, No. 3, 1991

A Method for On-Line Background Subtraction in Frequency Domain Fluorometry

Gregory D. Reinhart,[1,2] Pasquina Marzola,[3] David M. Jameson,[2,4] and Enrico Gratton[5,6]

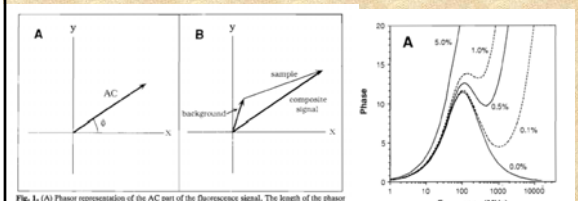

Fig. 1. (A) Phasor representation of the AC part of the fluorescence signal. The length of the phasor is proportional to the AC value, and the angle is equal to the phase angle as indicated. (B) Vector composition of background and sample signal to give the overall measured signal.

The phasor approach was dormant for many years until several laboratories began to apply it to FLIM

Tom Jovin
Andrew Clayton
Quentin Hanley ⇨ AB plots

Bob Clegg ⇨ polar plots

Enrico Gratton
Michelle Digman ⇨ phasor plots

More recently phasors have been applied to cuvette studies

Stefl, M., James, N.G., Ross, J.A. and Jameson, D.M. (2011) Anal. Biochem. 410:62-69. Application of Phasor to In Vitro Time-Resolved Fluorescence Measurements.

James, N.G., Ross, J.A., Stefl, M. and Jameson, D.M. (2011) Anal. Biochem. 410:70-76. Application of Phasor Plots to In Vitro Protein Studies.

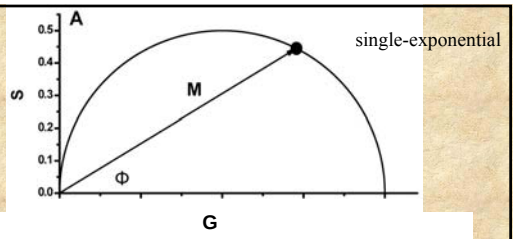

single-exponential

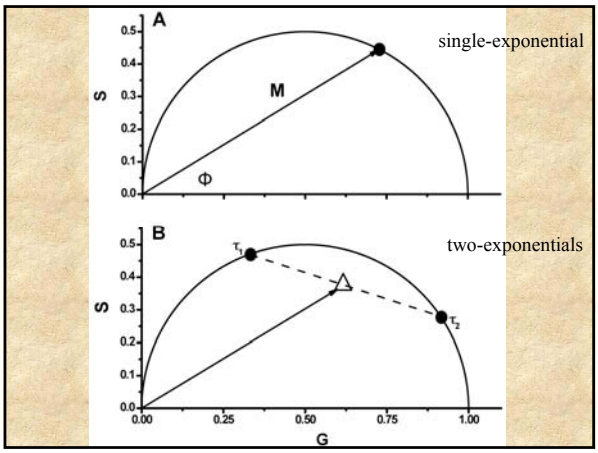

Methodological measurements I

- Map the position of the mixture of three different single-exponential dyes (Rhodamine B, AEDANS, DENS)

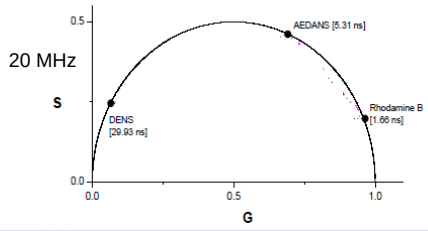

Methodological measurements I

- Map the position of the mixture of three different single-exponential dyes (Rhodamine B, AEDANS, DENS)
- The mixture lies inside the hypothetical triangle
- When some of the dye is added to the mixture – the point is moved towards the appropriate triangle vertex

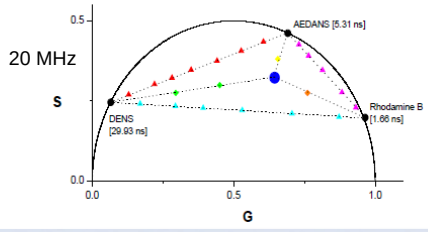

Methodological measurements II

- When analyzed for different frequencies – position of the hypothetical triangle in universal circle is anticlockwisely shifted when modulation frequency is increased
- Middle points copy the curvature of the universal circle

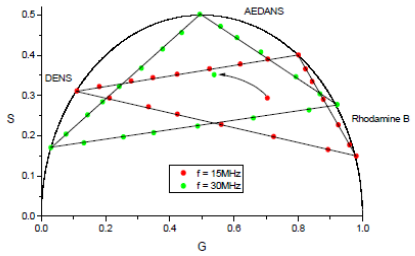

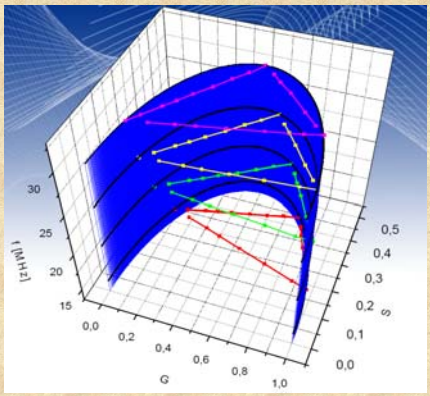

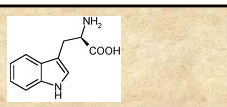

The pH dependent forms of tryptophan in solution are the zwitterionic and anionic forms due to the protonation of the amine and carboxyl groups – the pKa of the amine group is 9.39

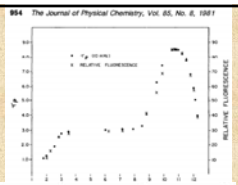

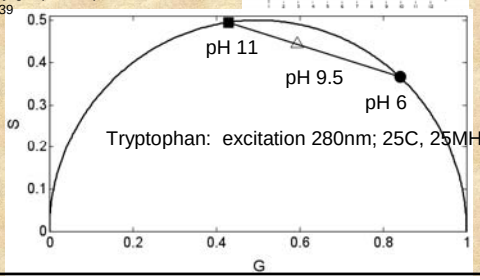

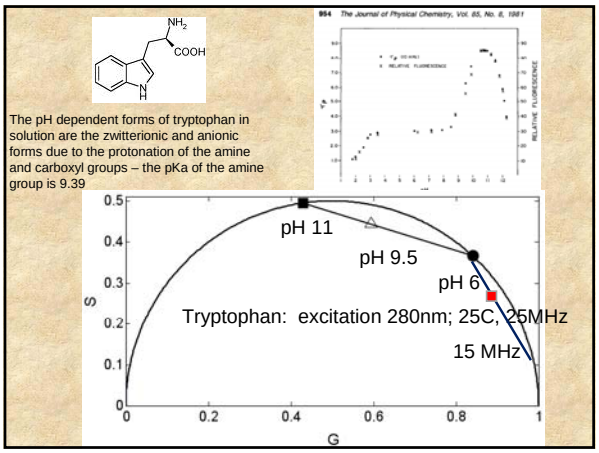
The pH dependent forms of tryptophan in solution are the zwitterionic and anionic forms due to the protonation of the amine and carboxyl groups – the pKa of the amine group is 9.39
pH 11
pH 9.5
pH 6
Tryptophan: excitation 280nm; 25C, 25MHz
15 MHz
S
G

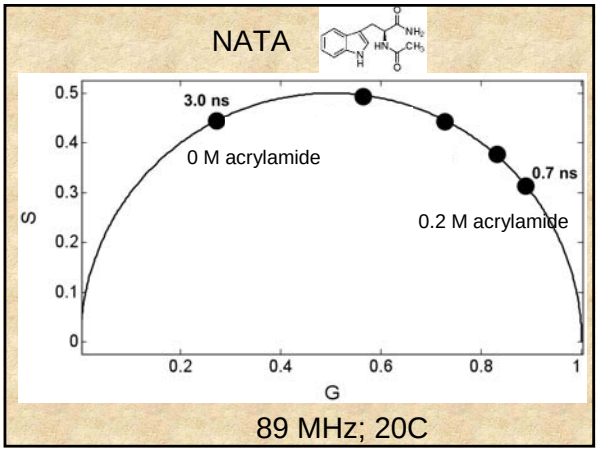
NATA
3.0 ns
0 M acrylamide
0.7 ns
0.2 M acrylamide
S
G
89 MHz; 20C

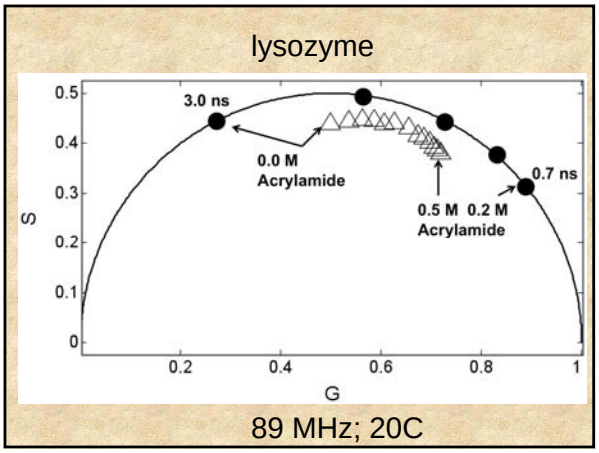
lysozyme
3.0 ns
0.0 M
Acrylamide
0.7 ns
0.5 M 0.2 M
Acrylamide
S
G
89 MHz; 20C

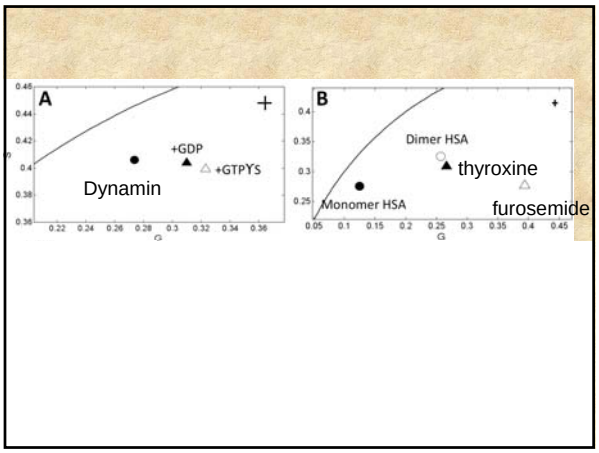

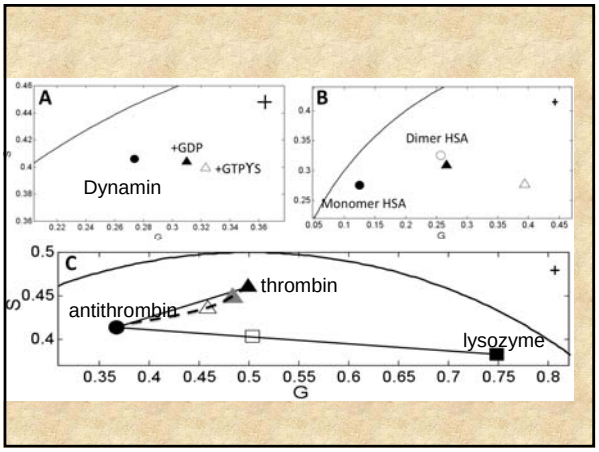

Kinetic phasor run on iron removal from the N-lobe of human transferrin

pH 6.0 with 4 mM EDTA over 300 seconds; 80 MHz

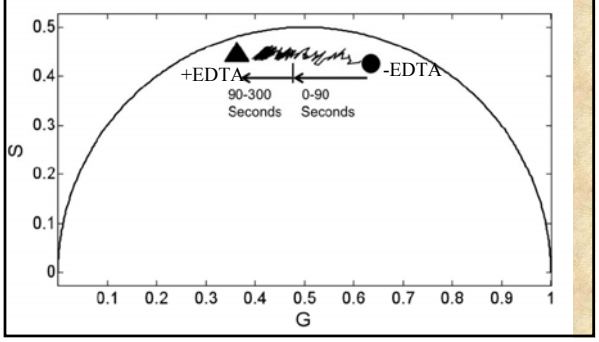

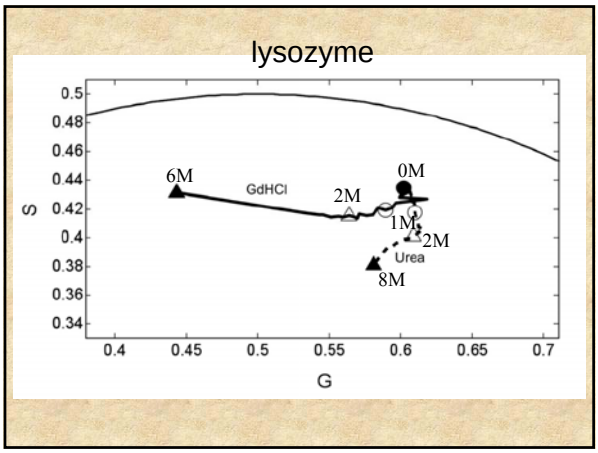
lysozyme
S
G
6M
GdHCl
2M
0M
1M
2M
Urea
8M

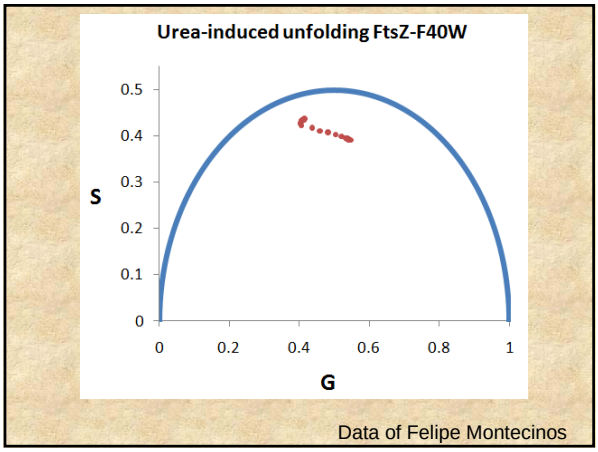
Urea-induced unfolding FtsZ-F40W
S
G
Data of Felipe Montecinos

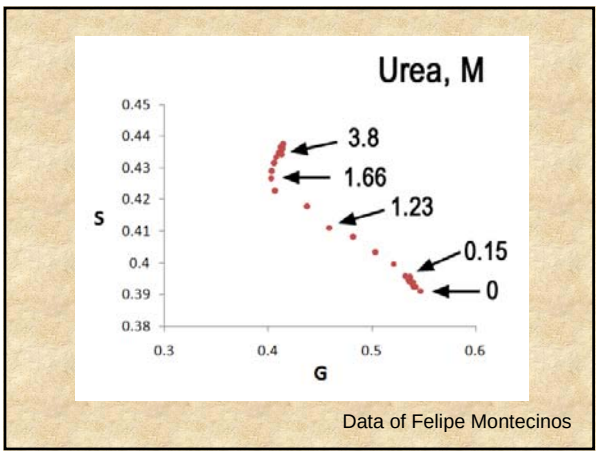
Urea, M
S
G
3.8
1.66
1.23
0.15
0
Data of Felipe Montecinos

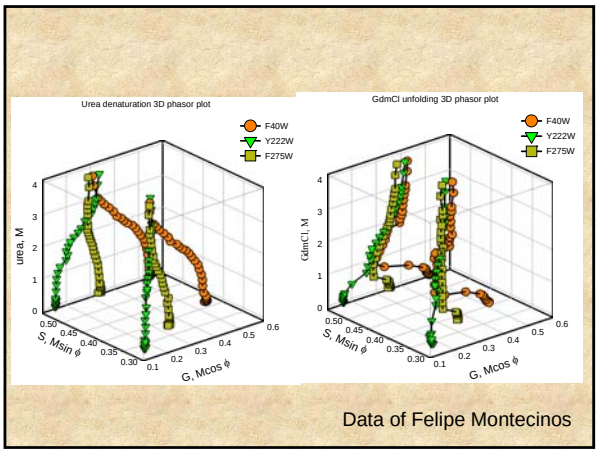
Urea denaturation 3D phasor plot
GdmCl unfolding 3D phasor plot
F40W
Y222W
F275W
urea, M
GdmCl, M
S, Msin ϕ
G, Mcos ϕ
Data of Felipe Montecinos

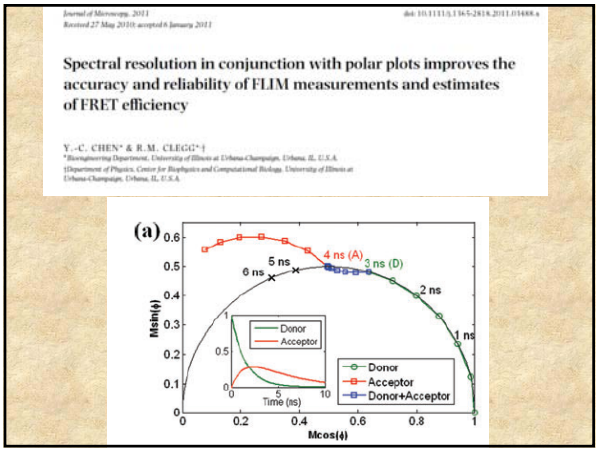
Spectral resolution in conjunction with polar plots improves the accuracy and reliability of FLIM measurements and estimates of FRET efficiency
Y.-C. CHEN* & R.M. CLEGG*†
(a)
6 ns
5 ns
4 ns (A)
3 ns (D)
2 ns
1 ns
Donor
Acceptor
Donor+Acceptor
Time (ns)
Msin(ϕ)
Mcos(ϕ)

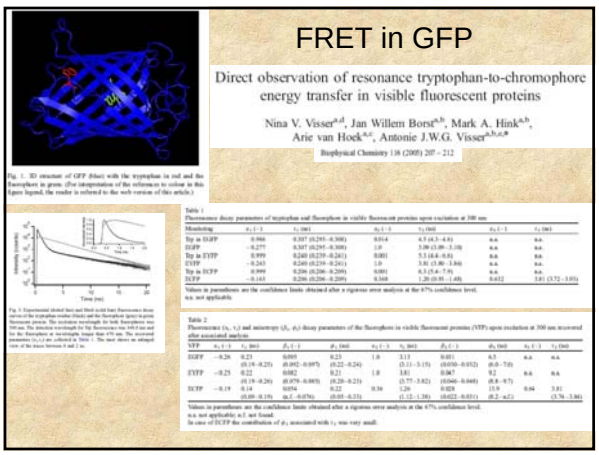
FRET in GFP
Direct observation of resonance tryptophan-to-chromophore energy transfer in visible fluorescent proteins
Nina V. Visser, Jan Willem Borst, Mark A. Hink, Arie van Hoek, Antonie J.W.G. Visser
Biophysical Chemistry 116 (2006) 207 – 212

FRET in GFP

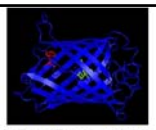

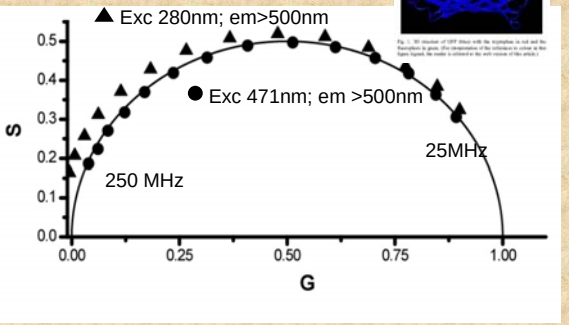

G-Quadruplex DNA are four stranded structures containing two or more stacked square-planar G-tetrads, composed of four Hoogstein hydrogen bonded guanines.

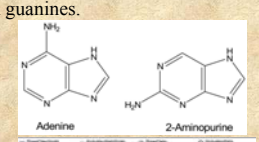

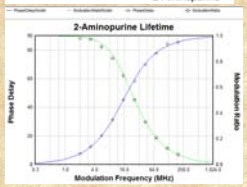

2-Aminopurine free in aqueous solution gives a single exponential lifetime of ~10 ns.

G-Quadruplex structure and stability illuminated by phasor plots
Robert Buscaglia, David M. Jameson and Jonathan B. Chaires
Nucleic Acid Research In Press

2-aminopurine Bases in Human Telomere Quadruplex Structures – Unique Environments for Each Position

1AP - 5`-**X**GGGTTAGGGTTAGGGTTAGGG
7AP - 5`-AGGGTT**X**GGGTTAGGGTTAGGG
13AP - 5`-AGGGTTAGGGTT**X**GGGTTAGGG
19AP - 5`-AGGGTTAGGGTTAGGGTT**X**GGG

Potassium and Sodium Phasors

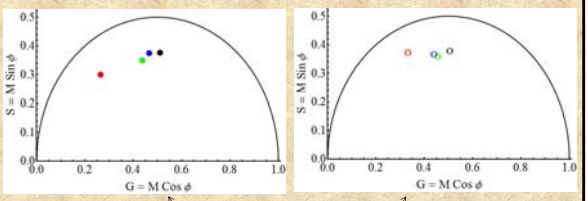

5'- AGGGTTAGGGTTAGGGTTAGGG
5'- AGGGTTAGGGTTAGGGTTAGGG
5'- AGGGTTAGGGTTAGGGTTAGGG
5'- AGGGTTAGGGTTAGGGTTAGGG

Substitution of potassium for sodium changes the structure and hence the lifetime of the 2-aminopurine Bases in Human Telomere Quadruplexex

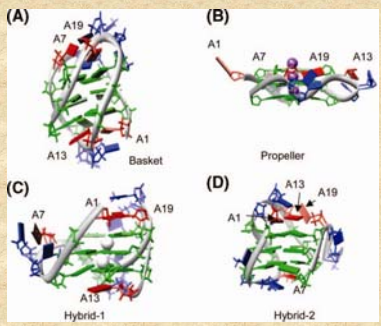

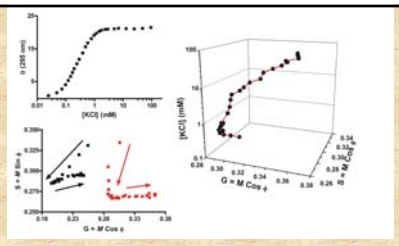

Figure 4. Monitoring changes to the 22-base G-Quadruplex forming sequence upon the addition of potassium using circular dichroism (top) and phasor plots (middle and bottom). (Top) Circular dichroism (Middle) Phasor representations at 93 MHz monitoring changes to the environment of 2-aminopurine for 1AP (black) and 13AP (red) G-Quadruplex forming sequences. Both substitutions show a sharp and fast phasor change between 0 to 5 mM potassium, with a slow change occurring from 5 to 100 mM. (Bottom) Three dimensional phasor representations at 93 MHz demonstrating the phasor points change direction above 1 mM potassium. Phasor representations are able to capture small changes during the folding of G-Quadruplex DNA upon the addition of cation and can be used to locally monitor specific loop regions.

G-Quadruplex structure and stability illuminated by phasor plots
Robert Buscaglia, David M. Jameson and Jonathan B. Chaires
Nucleic Acid Research In Press

Phasor approach to fluorescence lifetime microscopy distinguishes different metabolic states of germ cells in a live tissue

13582–13587 | PNAS | August 16, 2011 | vol. 108 | no. 33

Chiara Stringari[a], Amanda Cinquin[b,c], Olivier Cinquin[b,c], Michelle A. Digman[a], Peter J. Donovan[b,d], and Enrico Gratton[a,1]

[a]Laboratory of Fluorescence Dynamics, Biomedical Engineering Department, [b]Department of Developmental and Cell Biology, [c]Center for Complex Biological Systems, and [d]Department of Biological Chemistry and the Sue and Bill Gross Stem Cell Research Center, University of California, Irvine, CA 92697

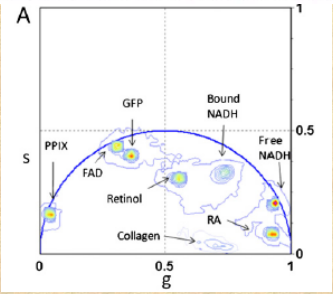

Time-Resolved Anisotropy and Excited State Reactions

Many of these slides were prepared by Theodore Hazlett

Time-resolved methodologies provide information on the changes of orientation as a function of time of a system. The time-domain approach is usually termed the **anisotropy decay** method while the frequency-domain approach is known as **dynamic polarization**. In principle both methods yield the same information.

In the time-domain anisotropy method the sample is illuminated by a pulse of vertically polarized light and the decay over time of both the vertical and horizontal components of the emission are recorded. The anisotropy function is then plotted versus time as illustrated here:

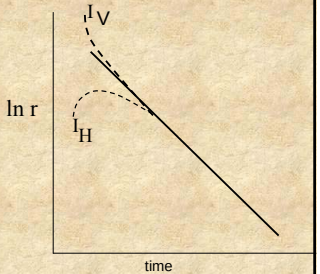

Note that the horizontal component actually increases during short times, since initially the fluorophores have not rotated significantly. As time passes though the number of horizontally oriented molecules increases

Simplest Case: Spherical Body

Fully Symmetrical

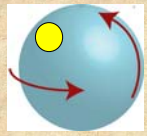

(in this case we assume that the fluorophore has no local mobility – such is the case for non-covalent interactions)

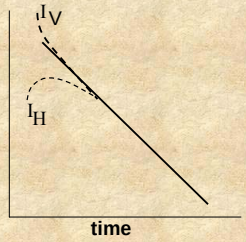

The decay of the anisotropy with time, r(t), for a sphere is given by:

$$r = \frac{Iv - Ih}{Iv + 2Ih} = r_o e^{-\left(t/\tau_c\right)}$$

τ_c is the rotational correlation time

$$\tau_c = \frac{1}{6 \cdot D_{rotation}}$$

In the case of non-spherical particles the time-decay of anisotropy function is more complicated. Mathematically simple symmetrical ellipsoids give us a sense of how changes in Shape affect the rotational diffusion rates.

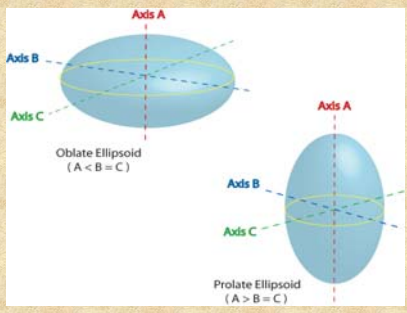

Effect of Shape on Diffusion

Translational Diffusion

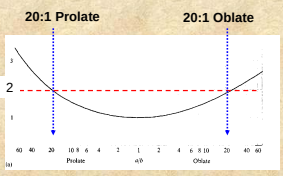

Rotational Diffusion

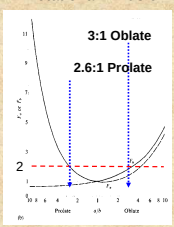

Rotational Diffusion is much more influenced by macromolecular shape than is Translational diffusion

How are these Shapes Modeled?

In the case of symmetrical ellipsoids of revolution the relevant expression is:

$$r(t) = r_1 e^{\left(\frac{-t}{\tau_{c1}}\right)} + r_2 e^{\left(\frac{-t}{\tau_{c2}}\right)} + r_3 e^{\left(\frac{-t}{\tau_{c3}}\right)}$$

where: $\tau_{c1} = 1/6D_2$

$\tau_{c2} = 1/(5D_2 + D_1)$

$\tau_{c3} = 1/(2D_2 + 4D_1)$

D_1 and D_2 are the rotational diffusion coefficients about the axes of symmetry and about either equatorial axis, respectively.

Resolution of the rotational rates is limited in practice to two rotational correlation times which differ by at least a factor of two.

What do the Anisotropy Amplitudes (r1, r2, & r3) Represent?

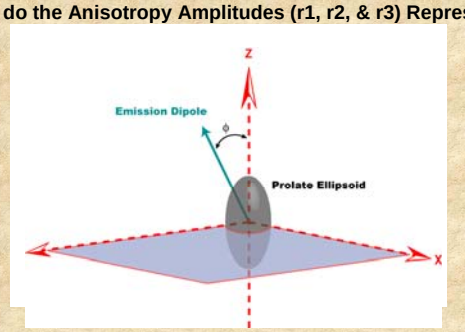

The amplitudes relate to orientation of the probe with respect to the axis of symmetry for the ellipsoid *(we are assuming colinear excitation and emission dipoles)*.

$r_1 = 0.1(3\cos^2\phi - 1)^2$
$r_2 = 0.3\sin^2(2\phi)$
$r_3 = 0.3\sin^4(\phi)$

Multiple Rotating Species (mixtures)

$$r(t) = r_1 e^{\left(\frac{-t}{\tau_{c1}}\right)} + r_2 e^{\left(\frac{-t}{\tau_{c2}}\right)}$$

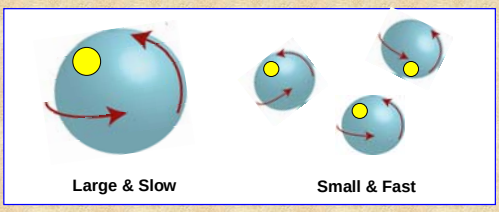

Large & Slow Small & Fast

Mixed systems Show Simple, Multi-Exponential Behavior

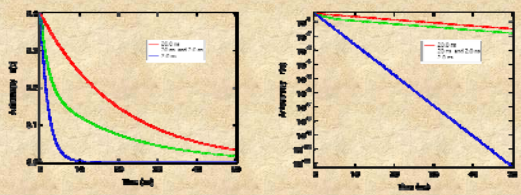

With separate species the decays reflect the sum of the exponential components present.

Multiple Rotational Modes: Local relaxation + Global rotation

Is the case of a **"local"** rotation of a probe attached to a spherical particle any different than multiple species?

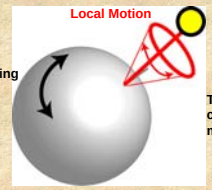

This common system represents a condition containing a hindered motion.

The expression for this case is:

$$r(t) = r_1 \cdot e^{-(t/\tau_{c1})} + r_2 \cdot e^{-(t/\tau_{c1} + t/\tau_{c2})}$$

Where τ_{c1} represents the "Global" probe motion, τ_{c2} represents the "Local" rotation of the macromolecule.

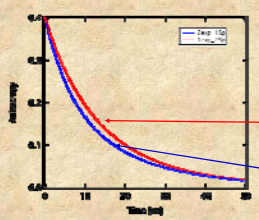

Equal pre-exponentials terms containing two rotational components of 20 ns and 10 ns

The "Mixed" case

The "Local & Global" case

Hindered Rotational Systems
Membrane Bilayers

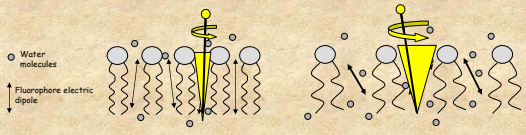

Wobble-in-a-Cone Concept

1) Freedom of motion
2) The rate of motion

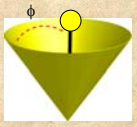

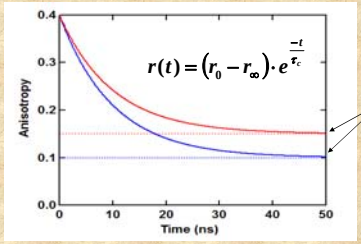

$r_{infinity}$

$$\frac{r_0}{r_\infty} = \left\langle \frac{3 \cdot \cos^2(\phi) - 1}{2} \right\rangle^2$$

Motion
τ_c = 20 ns

Angular Freedom
ϕ= 52 degrees
ϕ= 44 degrees

Analysis of Fluorophore Rotation in an Artificial Bilayer

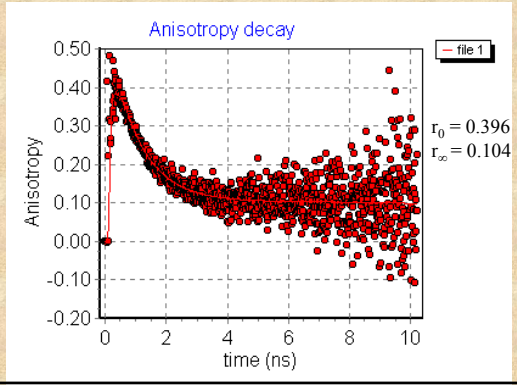

Phase & Modulation Measurements

In dynamic polarization measurements, the sample is illuminated with vertically polarized, modulated light. The phase delay (dephasing) between the parallel and perpendicular components of the emission is measured as well as the modulation ratio of the AC contributions of these components. The expressions a spherical particle are:

$$\Delta\phi = \tan^{-1}\left[\frac{18\omega r_o R}{\left(k^2+\omega^2\right)\left(1+r_o-2r_o^2\right)+6R\left(6R+2k+kr_o\right)}\right]$$

$$Y^2 = \frac{\left((1-r_o)k+6R\right)^2+\left(1-r_o\right)^2\omega^2}{\left[\left(1+2r_o\right)k+6R\right]^2+\left(1+2r_o\right)^2\omega^2}$$

Where $\Delta\phi$ is the phase difference, Y the modulation ratio of the AC components, ω the angular modulation frequency, r_o the limiting anisotropy, k the radiative rate constant ($1/\tau$) and R the rotational diffusion coefficient.

The illustration below depicts the $\Delta\phi$ function for the cases of spherical particles with different rotational relaxation times.

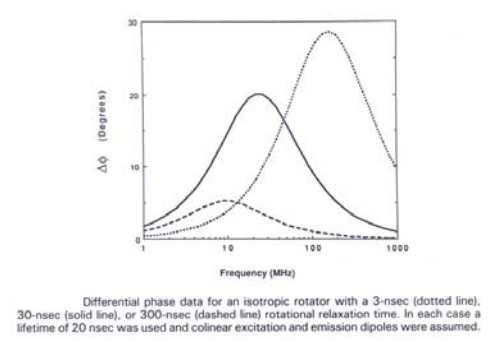

Differential phase data for an isotropic rotator with a 3-nsec (dotted line), 30-nsec (solid line), or 300-nsec (dashed line) rotational relaxation time. In each case a lifetime of 20 nsec was used and colinear excitation and emission dipoles were assumed.

The figures here show actual results for the case of ethidium bromide free and bound to tRNA - one notes that the fast rotational motion of the free ethidium results in a shift of the "bell-shaped" curve to higher frequencies relative to the bound case. The lifetimes of free and bound ethidium bromide were approximately 1.8 ns and 27 ns respectively.

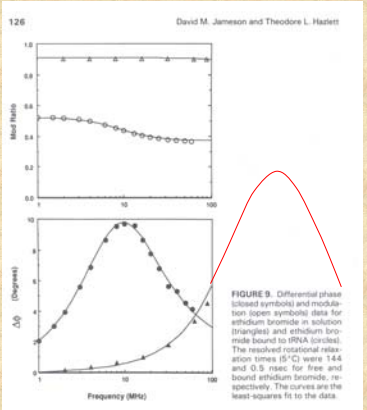

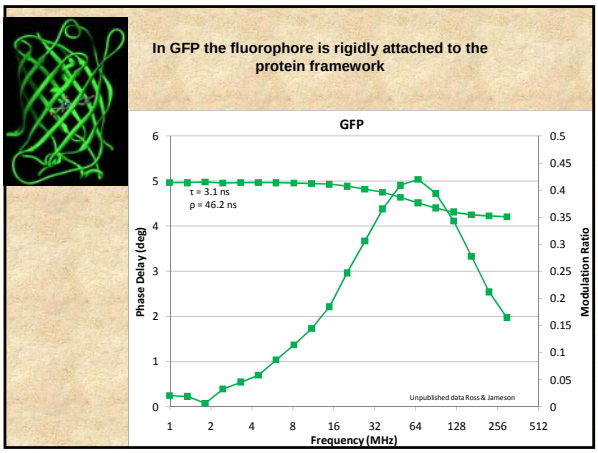
In GFP the fluorophore is rigidly attached to the protein framework
GFP
τ = 3.1 ns
ρ = 46.2 ns
Phase Delay (deg)
Modulation Ratio
Unpublished data Ross & Jameson
Frequency (MHz)

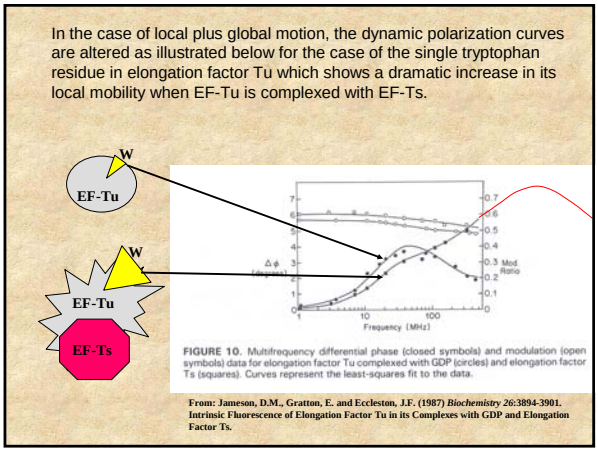
In the case of local plus global motion, the dynamic polarization curves are altered as illustrated below for the case of the single tryptophan residue in elongation factor Tu which shows a dramatic increase in its local mobility when EF-Tu is complexed with EF-Ts.
W
EF-Tu
W
EF-Tu
EF-Ts
Frequency (MHz)
FIGURE 10. Multifrequency differential phase (closed symbols) and modulation (open symbols) data for elongation factor Tu complexed with GDP (circles) and elongation factor Ts (squares). Curves represent the least-squares fit to the data.
From: Jameson, D.M., Gratton, E. and Eccleston, J.F. (1987) Biochemistry 26:3894-3901. Intrinsic Fluorescence of Elongation Factor Tu in its Complexes with GDP and Elongation Factor Ts.

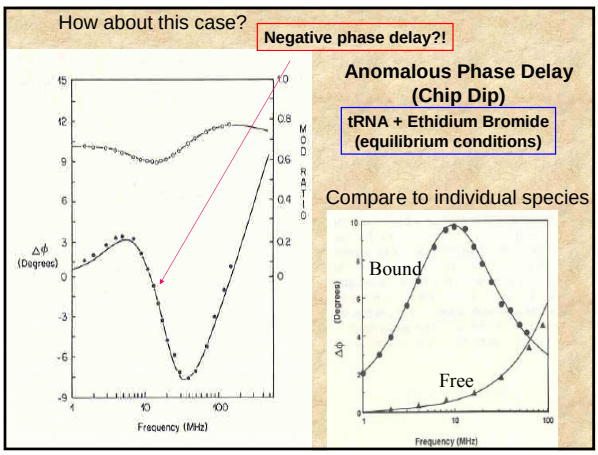
How about this case?
Negative phase delay?!
Anomalous Phase Delay (Chip Dip)
tRNA + Ethidium Bromide (equilibrium conditions)
Compare to individual species
Bound
Free
Frequency (MHz)

What do We have in Our Mixture?

+

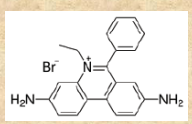

Ethidium Bromide

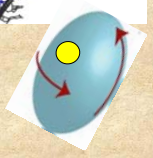

+

Slow rotation + long lifetime

Fast rotation + short lifetime

Time Domain Equivalent of the Anomalous Phase Delay

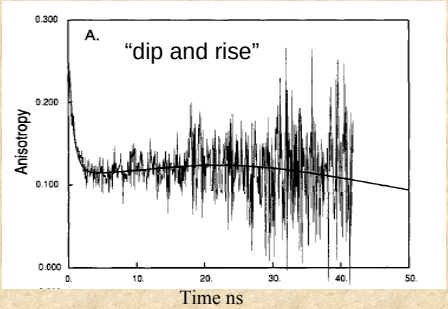

Guest et al., Interaction of DNA with the Klenow fragment of DNA polymerase I studied by time-resolved fluorescence spectroscopy. Biochemistry. 1991 Sep 10;30(36):8759-70.

Final comment: Although we have discussed analysis of rotational rates in terms of discrete components, in some cases a more realistic approach may be to use distribution functions

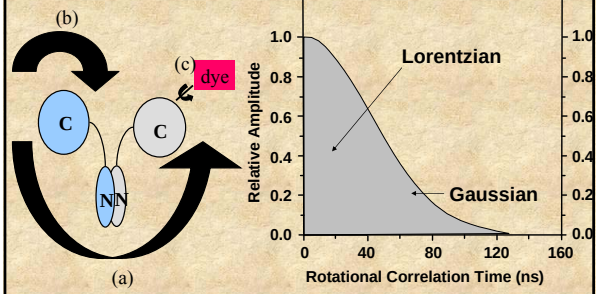

See: Analysis of anisotropy decays in terms of correlation time distributions, measured by frequency-domain fluorometry. Biophys Chem. 1994 Sep;52(1):1-13. Gryczynski I, Johnson ML, Lakowicz JR.

Quenching

A number of processes can lead to a reduction in fluorescence intensity, i.e., quenching

These processes can occur during the excited state lifetime – for example collisional quenching, energy transfer, charge transfer reactions or photochemistry – or they may occur due to formation of complexes in the ground state

We shall focus our attention on the two quenching processes usually encountered – namely collisional (dynamic) quenching and static (complex formation) quenching

Collisional Quenching

Collisional quenching occurs when the excited fluorophore experiences contact with an atom or molecule that can facilitate non-radiative transitions to the ground state. Common quenchers include O_2, I^-, Cs^+ and acrylamide.

In the simplest case of collisional quenching, the following relation, called the **Stern-Volmer equation**, holds:

$$F_0/F = 1 + K_{SV}[Q]$$

where F_0 and F are the fluorescence intensities observed in the absence and presence, respectively, of quencher, [Q] is the quencher concentration and K_{SV} is the **Stern-Volmer quenching constant**

In the simplest case, then, a plot of F0/F versus [Q] should yield a straight line with a slope equal to K_{SV}.

Such a plot, known as a Stern-Volmer plot, is shown below for the case of fluorescein quenched by iodide ion (I^-).

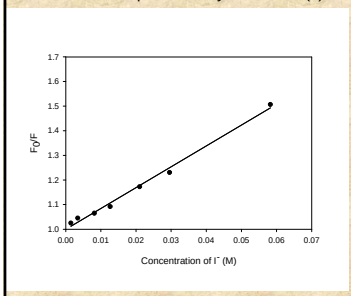

In this case, K_{SV} ~ 8 L-mol^{-1}

$K_{SV} = k_q \tau_0$ where **k_q is the bimolecular quenching rate constant** (proportional to the sum of the diffusion coefficients for fluorophore and quencher) and **τ_0 is the excited state lifetime** in the absence of quencher.

In the case of purely collisional quenching, also known as ***dynamic*** quenching,:

$$F_0/F = \tau_0/\tau.$$

Hence in this case: $\tau_0/\tau = 1 + k_q \tau[Q]$

In the fluorescein/iodide system, τ = 4ns and k_q ~ 2 x 10^9 M^{-1} sec^{-1}

Why does dynamic quenching reduce the lifetime?

Recall:

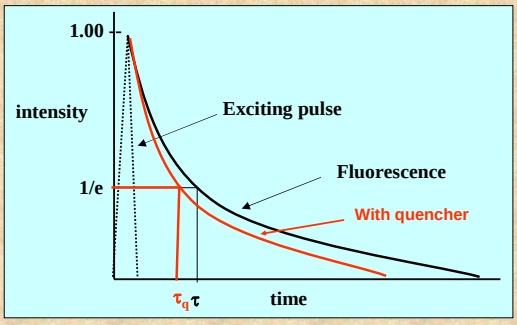

Static Quenching

In some cases, the fluorophore can form a stable complex with another molecule. If this *ground-state* is non-fluorescent then we say that the fluorophore has been statically quenched.

In such a case, the dependence of the fluorescence as a function of the quencher concentration follows the relation:

$$F0/F = 1 + Ka[Q]$$

where Ka is the association constant of the complex. Such cases of quenching via complex formation were first described by Gregorio Weber.

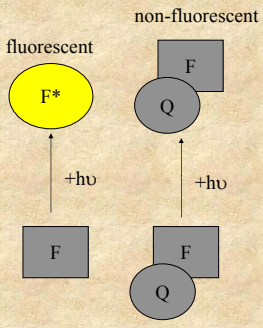

If both static and dynamic quenching are occurring in the sample then the following relation holds:

$$F_0/F = (1 + k_q \tau[Q])\,(1 + K_a[Q])$$

In such a case then a plot of F_0/F versus [Q] will give an upward curving plot

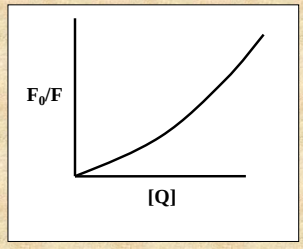

The upward curvature occurs because of the $[Q]^2$ term in the equation

However, since the lifetime is unaffected by the presence of quencher in cases of pure static quenching, a plot of τ_0/τ versus [Q] would give a straight line

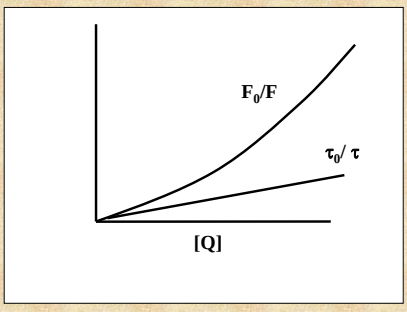

Sometimes you will see the equation for simultaneous static and dynamic quenching given as:

$$F_0/F = (1 + K_{SV}[Q])e^{V[Q]}$$

where the term $e^{V[Q]}$ is used as a phenomological descriptor of the quenching process. The term V in this equation represents an *active volume* element around the fluorophore such that any quencher within this volume at the time of fluorophore excitation is able to quench the excited fluorophore.

Non-linear Stern-Volmer plots can also occur in the case of purely collisional quenching if some of the fluorophores are less accessible than others. Consider the case of multiple tryptophan residues in a protein – one can easily imagine that some of these residues would be more accessible to quenchers in the solvent than other.

In the extreme case, a Stern-Volmer plot for a system having accessible and inaccessible fluorophores could look like this:

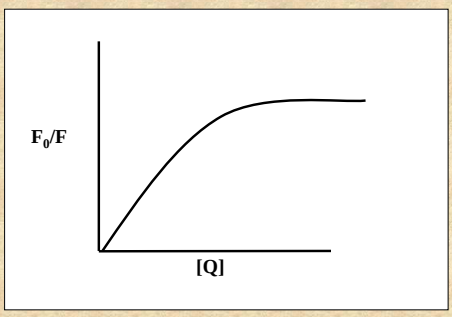

The quenching of LADH intrinsic protein fluorescence by iodide gives, in fact, just such a plot. LADH is a dimer with 2 tryptophan residues per identical monomer. One residue is buried in the protein interior and is relatively inaccessible to iodide while the other tryptophan residue is on the protein's surface and is more accessible.

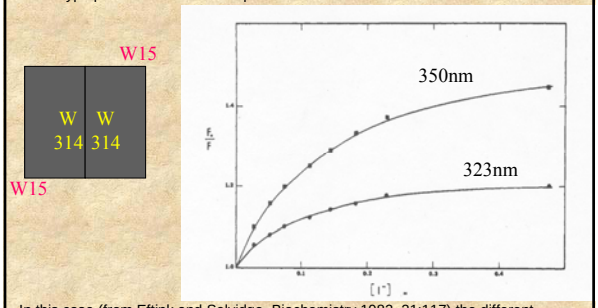

In this case (from Eftink and Selvidge, Biochemistry 1982, 21:117) the different emission wavelengths preferentially weigh the buried (323nm) or solvent exposed (350nm) tryptophans.